JOURNAL OF GEOPHYSICAL RESEARCH, VOL. 104, NO. B3, PAGES 4887–4899, MARCH 10, 1999

Recent crustal deformation in southern California deduced from the restoration of folded and faulted strata

J. P. Gratier,[1] T. Hopps,[2] C. Sorlien,[3] and T. Wright[4]

Abstract. A rigid element method of restoration (UNFOLD) is used to restore competent folded and faulted layers of the Ventura and Los Angeles basins to their initial horizontal state. Comparison of initial (undeformed) state with present (deformed state) allows one to estimate both the finite crustal deformation and its associated horizontal displacement field (relative to an arbitrary fixed line). Including data from the Santa Barbara Channel basin, the total finite displacement field for the western Transverse Ranges and vicinity (within the Pacific plate) is inferred from this map restoration and is modeled as a double fan closure. This model implies a 10° clockwise rotation of the northern boundary of the western Transverse Ranges and a 5° counterclockwise rotation of its northeast boundary. Lateral variation of the deformation reveals the heterogeneity of the subsurface deformation. Most of the major thrusts appear to initiate as en echelon structures along the left-lateral northern margin and the right-lateral northeastern margin of the studied area. The resulting deformation and displacement values closely match those derived by other geological methods (section balancing techniques or fault slip measurements) and by geophysical methods (geodetic, paleomagnetic, and focal mechanism data). Map restoration thus is a method that can independently quantify both local and regional deformation including folds and faults. This method also reveals the zones where problems of compatibility appear with the available geological and geophysical data and thus where the next studies might be focused.

1. Introduction

As it becomes increasingly important to better understand seismic hazards in southern California, modeling recent crustal deformation is needed to forecast the future behavior of active faults in this region. Such mechanical modeling implies the knowledge of three types of parameters: (1) the boundary conditions (displacement field around the faults), (2) the rheology of the rocks, and (3) the thermodynamic conditions (stress, temperature, nature, and pressure of fluids). Our knowledge of these parameters is rather poor; consequently, the reliability of the models is strongly dependent on their improvement. Estimating the recent deformation and displacement field in this area of active faulting is thus a major task and the main object of this work.

Modern displacements are estimated from geodetic data [*Larson and Webb*, 1992; *Feigl et al.*, 1993; *Donnellan et al.*, 1993; *Larsen et al.*, 1993; *Shen et al.*, 1996]. However, instantaneous deformation of the surface is not necessarily directly representative of the recent crustal deformation associated with major active faults both because of possible local effects (gravity sliding) and of possible irregular evolution of the deformation rate with time (partition between reversible and irreversible deformation during the earthquake cycle). Kinematic models which include geological displacement values on major faults [*Bird and Rosenstock*, 1984; *Weldon and Humphreys*, 1986; *Humphreys and Weldon*, 1994; *Bird and Kong*, 1994] allow the finite displacement to be integrated over long periods of time. However, uncertainty on the displacement values associated with, for example, blind faults limits the accuracy of the models. Rotations are accurately estimated by paleomagnetic data, but most measurements represent 10–20 million years averages [*Luyendyk*, 1991].

The idea of this work is to use the folded and faulted sedimentary cover as markers of progressive crustal deformation in order to estimate the irreversible finite horizontal deformation and displacement field within a deformed area. When, as is the case in southern California, sediment deposits occur in a tectonically active region, the deformed strata can be used as strain gauges of the progressive deformation. If the present geometry of a reference deformed layer is well known and if this layer may be restored to its initial state (assumed to be horizontal), comparison between present (deformed) state and restored (undeformed) state allows one to estimate the finite deformation (e.g., horizontal shortening of folded and faulted blocks) and the associated total finite horizontal displacement (e.g., displacement of points with respect to a reference line). Uncertainty may appear if the sedimentary deposits are not perfectly horizontal before the deformation; however, because of the large values of the deformation in the Transverse Ranges, this uncertainty is very low. As with geodetic data, the displacement field is estimated by reference to an arbitrary fixed line.

2. Method

Two types of method may be used to estimate heterogeneous deformation. The first one is to partition the whole deformed area into homogeneous domains, then to restore and best fit all these domains in order to reconstitute the initial

[1]Laboratoire de Geophysique Interne et Tectnophysique (LGIT), CNRS-Observatoire, Université Joseph Fourier, Grenoble, France.
[2]Rancho Energy Consultants, Santa Paula, California.
[3]Institute for Crustal Studies, University of California, Santa Barbara.
[4]San Anselmo, California.

Paper number 1998JB900049.
0148-0227/99/1998JB900049$09.00

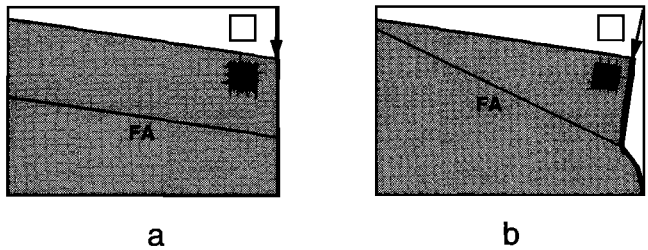

Figure 1. Map view of two different models for oblique folding in an arcuate fold belt. The open area is the initial state; the shaded area is the deformed state. Strain markers: open square is the initial state, and black square is the final strain (constant volume) either by (a) distortion or by (b) rigid rotation, FA is the map trace of the fold axis. Figure 1a shows the simple shear deformation with constant area in cross sections parallel to the displacement (arrow) and parallel to the layer distortion (with change in angle between two lines). This model is used in the balanced cross section technique. Figure 1b shows the developable folding with rigid rotation of the fold limb but no distortion of the layer in the limbs of the fold (with no change in angle between two lines parallel to the layer). This model is used in the UNFOLD technique.

undeformed state [*Oertel*, 1974; *Schwerdtner*, 1977; *Cobbold*, 1979]. Regional removal of ductile strain [*Cobbold and Percevault*, 1983] and restoration of the folded foreland of a mountain range [*Gratier et al.*, 1989] have been done by this method. Another type of method, used here, is to directly restore the folded and faulted layers using a rigid element method of restoration (UNFOLD program) [*Gratier et al.*, 1991]. Layers are restored just as folded and torn sheets of paper may be smoothed with an iron. Moreover, this type of program allows one to test the geometric compatibility of the data since a balanced folded and faulted layer must be restorable to its initial state. As for the cross-section balancing technique, this map balanced restoration is founded on basic assumptions concerning the mechanical behavior of the studied layers. UNFOLD assumes that the mapped layers are folded and faulted without significant change in thickness of the strata and without change in length along the folded surface (Figure 1b). The section-balancing technique has been successful in projecting geological structures with depth [*Dahlstrom*, 1969; *Hossack*, 1979; *Suppe*, 1983]. However, as balanced cross sections must be constructed parallel to the plane of constant area, the cross-section technique is limited either to cylindrical fold/fault structures or, more generally, to structures with parallel horizontal displacement. In this case (Figure 1a), horizontal rotation of fold axes requires fold limb distortion (change in angle between two lines). In contrast, UNFOLD permits nonparallel displacement (Figure 1b), and fold axis rotation is linked to a rigid rotation of the limbs of the folds (no change in angle between two lines).

The UNFOLD procedure [*Gratier et al.*, 1991; *Gratier and Guillier*, 1993] includes the following steps. The folded and faulted area is divided into blocks bounded by faults or by arbitrary boundaries. Each folded block is digitized from structure contour maps or cross sections. These data are interpolated by spline functions using the Generic Mapping Tools (GMT) system [*Wessel and Smith*, 1991] in order to obtain a three-dimensional XYZ network of points with a regular Cartesian XY grid (Figure 2a). The grid points are organized into rigid triangular elements, the size of these rigid elements being as small as possible to best fit the fold geometry. These triangular elements are successively laid flat column by column and best fitted by a least squares method [*Etchecopar*, 1977]. Each triangular element is fitted into the triangular hole defined by its neighbors. For each pair of triangles (element/hole) a fitting value (f) is estimated as the ratio D/M, D being the distance between the vertices of each triangle and those of the hole it is fitting in and M being the mean value of the three medians of the triangles. A mean value of the fitting indicator (F) can also be expressed for the whole surface. After a first fitting of all the triangles, an approximate initial state is estimated. Fittings are repeated until a minimum mean value of the fitting indicator F is attained. During each iteration the new position of each triangle is used to fit the following one.

If the folded layer is a developable surface, with no thickness change or layer-parallel stretching like a sheet of paper, the misfit of the triangle must be as low as possible and the mean-fitting indicator value (F) progressively decreases to a minimum low value (about 0.005 for the unfolding of folded sheets of paper) [see *Gratier et al.*, 1991]. The fitting indicators can be used to estimate the reliability of the unfolding. In natural deformation, competent layers are most likely to behave as developable layers, and field observations can be used to test this presumption. When considering layers that are in reality developable, poor-fitting indicator values indicate that the structure-contour map does not accurately represent the

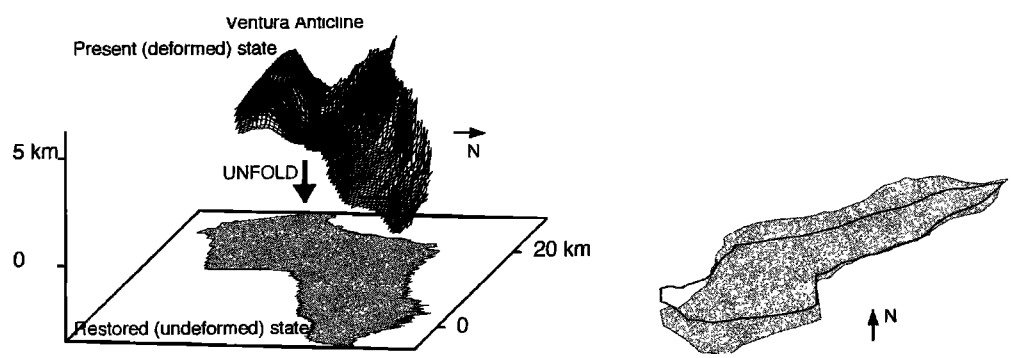

Figure 2. Two steps of the UNFOLD program applied to the example of Ventura Avenue anticline. (a) Perspective view of the present deformed state digitized from structure contour maps (top) and restored undeformed state (bottom) by the UNFOLD program. The folded blocks are limited by faults, or arbitrary boundaries. The size of the ridge elements is 200 × 200 m. (b) The map view after unfolding and the comparison between the initial unfolded block (shaded area) and its present deformed state (open area) are shown.

folded layers. When satisfactory fitting indicator values are obtained [*Gratier et al.*, 1991], comparison of the present (deformed) and initial (undeformed) state for each block gives the finite deformation for each of these blocks (Figure 2b, 4). Following *Ramsay* [1967], this deformation is represented as a horizontal strain ellipse. The determination of the values of the principal strain ratio and orientation of the axes of such a strain ellipse is done by comparing the geometry of the map projection of the deformed block with that of the restored block. The two blocks are superposed and the distances between each common points and the superposed barycenter of the blocks are estimated. The plots of the variation in elongation values versus the variation in direction values give the shape and orientation of the strain ellipse.

After being successively restored to their initial horizontal state, the unfolded blocks are best fitted together using an interactive graphics program. Assuming constant thickness, difficulty in obtaining a good fit along the fault cutoffs indicates some mismatches between the geometry of the footwall and those of the hanging wall of the fault (i.e., mistake in the amount of overthrust or associated vertical axis rotation). After being modified, if necessary by reinterpreting the data, a balanced geometry of the layer is obtained [*Gratier and Guillier*, 1993]. Assuming an arbitrary fixed line, comparison of the present (deformed) state with the restored (undeformed) state gives the total finite displacement field and the total finite horizontal deformation of the entire studied area, including folds and faults.

Finally, the idea of this work is not to establish a definitive model of the kinematics of southern California. Instead, the main interest of the restoration method is to impose a geometric and kinematic compatibility between the data. As new data become available, the reconstruction can be modified, and the interpretations of the data can be subjected to this map-based kinematic test. Numerous petroleum wells result in highly controlled structure-contour maps and cross sections of the folded and faulted sedimentary cover in the Los Angeles, Ventura, and Santa Barbara Channel basins and allow us to establish a basic structural pattern that is compatible with geometric data in three dimensions. The finite displacement field inferred from restoring the structure-contour maps is compatible with the results of other geophysical and geological methods but adds additional information on the progressive crustal deformation (e.g., strain values along strike and vertical axis block rotation). Map restoration can independently quantify both local and regional block rotation, finite deformation, and finite displacement. This method also reveals zones where compatibility is problematic and where the next studies might be focused. When the geometry of superimposed syndeformation layers is available, the kinematics of the deformation may be obtained by the restoration of such variably deformed layers [*Gratier and Guillier*, 1993]; however such a data set was not available in the studied areas.

3. Tectonic Setting and Timing of the Deformation

The Neogene deformation of the studied area is associated with the development of the western Transverse Ranges and of the major transcurrent faults related to the San Andreas fault system [see *Crowell*, 1981; *Molnar*, 1993; *Powell*, 1993; *Weldon et al.*, 1993] (Figure 3). Today, the western Transverse Ranges province is characterized by E-W-oriented faults and folds, anomalous to the regional NW-SE trend of the San Andreas fault zone. This province is bisected by the elongate Ventura and Santa Barbara Channel basins and bounded to the north by the Santa Ynez fault and Santa Maria basin, to the south by the Santa Monica-Santa Cruz Island faults and Los Angeles basin, to the east by the San Gabriel fault and Ridge basin, and to the west by the Hosgri fault system (Figure 3).

The progressive late Cenozoic deformation in the western Transverse Ranges and in its neighboring basins was rather complex. Regional clockwise vertical-axis rotation (90°) of the western Transverse Ranges province was initiated during early Miocene time and was accompanied by major extension [*Luyendyk*, 1991; *Crouch and Suppe*, 1993]. This evolution is associated with the capture of microplates by the Pacific plate and the subsequent development of the major transcurrent faults of the San Andreas system [*Crowell*, 1981; *Lonsdale*, 1991; *Atwater*, 1989; *Nicholson et al.*, 1994]. Extensional or transtensional basins were superimposed on the older forearc basin, and volcanic and terrigenous deposition occurred around the basin margins, followed by, or synchronous with, biogenic deposition within starved parts of the basins. At least some of these early normal faults were reactivated as thrust or oblique-reverse faults at, or after, the end of Miocene time [*Clark et al.*, 1991; *Huftile and Yeats*, 1996; *Sorlien et al.*, 1999; L. Seeber and C. C. Sorlien, Listric thrusts in the Western Transverse Ranges, California, submitted to *Geological Society of America. Bulletin*, (hereinafter referred to as Seeber and Sorlien, submitted manuscript, 1998)]. Rates of terrigenous sedimentation increased by at least an order of magnitude, especially within the rapidly subsiding Ventura and Los Angeles basins. Most of the maps we restored are on horizons affected only by the late period of horizontal contraction that induced folds and thrust faults ~4–5 million years ago, with an uncertainty of 1 or 2 million years (see discussion by *Molnar* [1993]). Unfolding of two layers of different age, 4.5 Ma and 14 Ma (14 Ma restoration not shown here), in the Los Angeles basin shows no significant difference in the deformation field. This indicates that the shortening process could not have started long before the youngest horizon (4.5 Ma) and that major extension predates 14 Ma.

Initiation of this contraction was about 5 Ma in offshore Santa Maria basin and along the northern margin of Los Angeles basin [*Clark et al.*, 1991; *Hummon et al.*, 1994; *Schneider et al.*, 1996]. Accelerated shortening across onshore and offshore Santa Maria basin and Santa Barbara Channel dates from ~3 or 4 Ma [*Clark et al.*, 1991; *Edward and Heck*, 1994; *McGroder et al.*, 1994] and is also inferred by Seeber and Sorlien (submitted manuscript 1998), using *Dumont and Barron* [1995]. Cross sections in *Wright* [1991] indicate that strata deposited during Repettian stage, including the lowermost strata, thin onto folds along the northern margin of the Los Angeles basin, while folding occurred near the end of the Repettian stage in the south of that basin. Although the Repettian stage can be time-transgressive, its base is ~4.5 Ma [*Wright*, 1991] or 5 Ma [*Blake*, 1991], and its top is ~2.5 Ma in the Los Angeles basin [*Blake*, 1991]. The timing of initial shortening across the Ventura basin is more elusive, in part because a phase of intense contraction within the basin that started at ~1 Ma has overprinted earlier deformation [*Yeats*, 1988; *Huftile and Yeats*, 1995]. However, thickness changes within the Fernando Formation are consistent with contraction as early as 5 Ma [*Yeats et al.*, 1994; *Huftile and Yeats*, 1996].

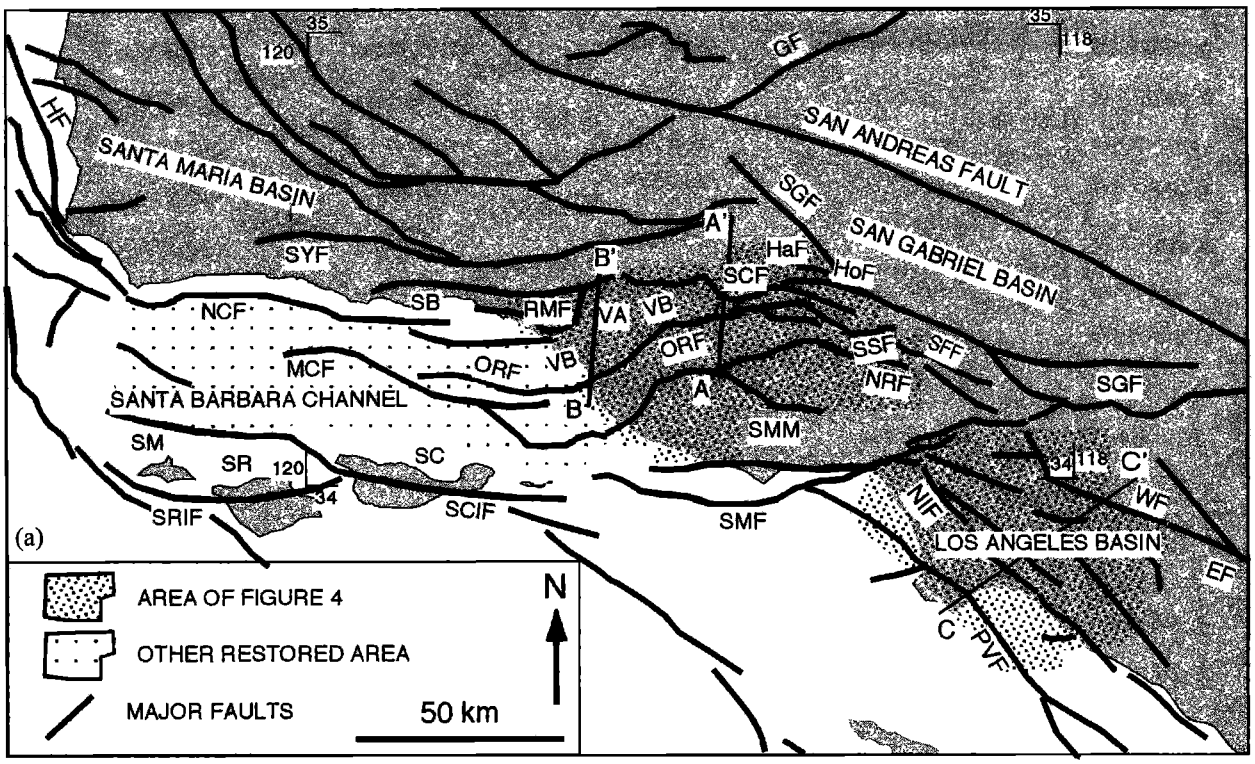

Figure 3. General structural features of the studied area. (a) Schematic structural map with location of the main structures: Channel Islands (San Miguel (SM), Santa Rosa (SR), and Santa Cruz (SC)), Channel Island faults (Santa Cruz Island fault (SCIF) and Santa Rosa Island fault (SRIF)), Elsinore fault (EF), Garlock fault (GF), Hasley fault (HaF), Hosgri fault (HF), Holser fault (HoF), Mid-Channel fault (MCF), Newport-Inglewood fault (NIF), North Channel fault (NCF), Northridge fault (NRF), Oak Ridge fault (ORF), Palos Verdes. (PVF), Red Mountain fault (RMF), San Andreas fault (SAF), San Gabriel fault (SGF), San Fernando fault (SFF), Santa Barbara (SB), Santa Cayetano fault (SCF), Santa Monica fault (SMF), Santa Monica Mountains (SMM), Santa Susana fault (SSF), Santa Ynez fault (SYF), Ventura Avenue Anticline (VA), Ventura Basin (VB), and Whittier fault (WF). (b) Schematic cross sections through the Ventura and Los Angeles basins, base of Saugus Fm (1 Ma) (dotted line), base of Repetto Fm (4.5 Ma) (dashed line), and base of Sespe Fm (35 Ma) (solid line). Section AA′ and BB′ were adapted from *Huftile and Yeats* [1995, 1996] and section CC′ was adapted from *Wright* [1991]. Perspective view of the Ventura Anticline is shown in Figure 2 in its present and restored state.

4. Data

The basins of southern California are rich in petroleum and therefore abundant well and seismic reflection data exist, along with subsurface maps and cross sections synthesized from these data. In the Los Angeles basin, two horizons have been mapped by correlations between numerous wells (Figure 4a): base of Repetto (4.5 Ma) and base of Mohnian stage (14 Ma). The structure contour maps of these two horizons are given by *Wright* [1991].

In the Ventura basin (Figure 4b) we used a set of structure contour maps and cross sections developed by R. J. Hindle et al. (unpublished document, 1989) and *Hopps et al.* [1995] and constructed by correlating time horizons, structure, stratigraphy, and well logs from over a thousand industry wells throughout the basin. The data set includes 17 subsurface structure contour maps of various horizons that are tied together in a grid of 21 structure cross sections. The result is a three-dimensional presentation of high-quality subsurface data that have been assembled and reconciled into a coherent geological

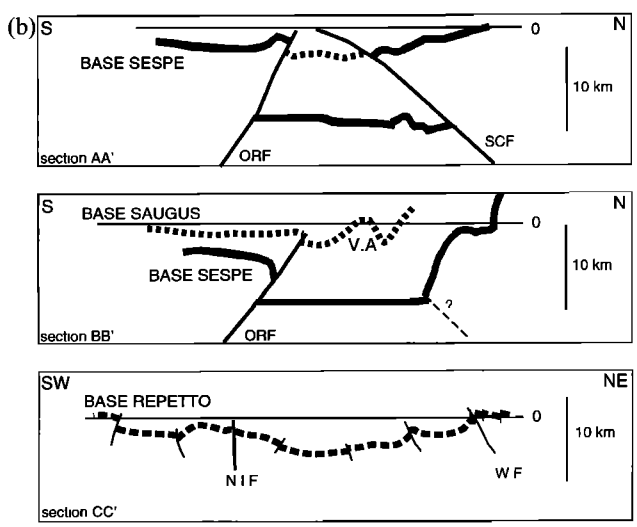

Figure 3. (continued)

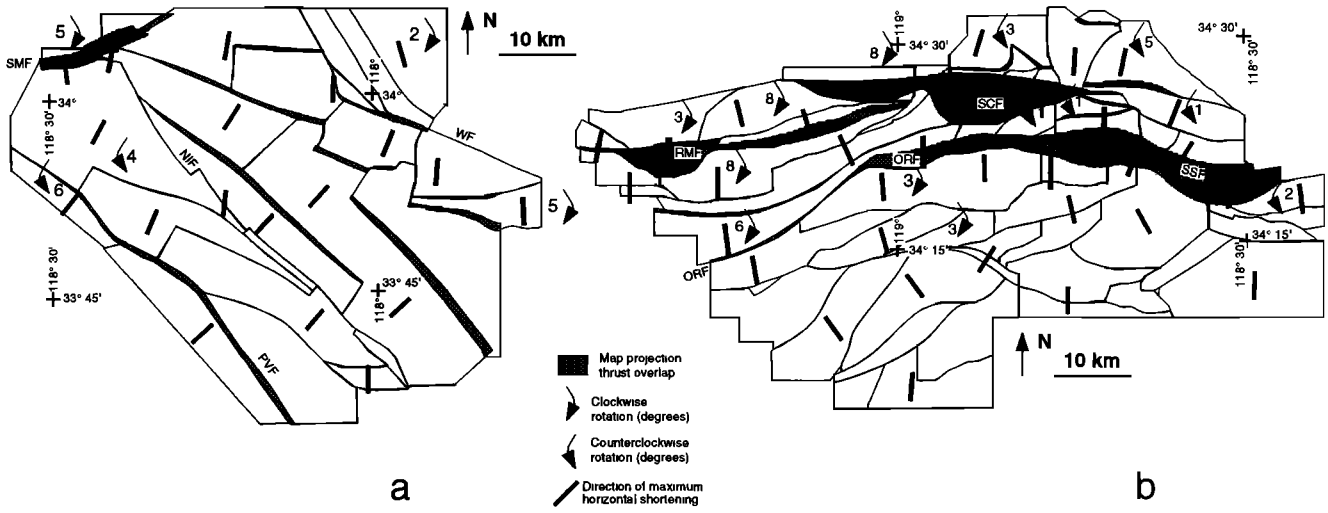

Figure 4. Present state of the (a) Los Angeles and (b) Ventura basins (see location in Figure 3), with indication of the finite deformation and rotation of the different blocks after unfolding. The gray area is the map projection of the thrust overlap of a 5 Ma horizon. In the east Ventura basin, several thrusts are superposed, which have not been distinguished on this schematic view. The maximum shortening directions are obtained by the unfolding of each block. The rotations are needed for the best fit of the unfolded blocks in the restored state.

interpretation. This data set cannot be represented in this paper for lack of space. However, the whole data set can be viewed at http://www.crustal.ucsb.edu/hopps [*Hopps et al.*, 1995; *Nicholson et al.*, 1997]. Full-sized hard copies of the maps and cross sections are still proprietary but are also available for research purposes under signed agreement from the Institute for Crustal Studies. In the Santa Barbara channel a map of the top of the Monterey Formation constructed by Grant McHattie et al. (Mobil Oil Co.) was evaluated and modified and then restored [C. C. Sorlien et al. Map restoration of folded and faulted late Cenozoic strata across the Oak Ridge fault, onshore and offshore Ventura basin, California, submitted *Geological Society of America Bulletin*, 1998 (hereinafter referred to as Sorlien et al., submitted manuscript, 1998)], and the result was integrated in this regional work. Because of the effect of the erosion, horizons of different age had to be used in the western part of the Ventura basin: Chatsworth formation (70 Ma), Llajas formation (45 Ma), top Sespe Formation (25 Ma), top Modelo Formation (5 Ma), top Pico (or Fernando) Formation (0.7–1 Ma) [*Dibblee*, 1982; *Yeats*, 1988]. Since structure contour maps of top Modelo (5 Ma) were available in the eastern part of the basin, the geometry of deformed layers of different ages in the western part was corrected in order to define the geometry of the top Modelo, 5 Ma horizon. For example, where the top Sespe Formation was mapped to the hanging wall cutoff and the top of the Pico Formation was mapped to the footwall cutoff across a thrust fault, the restoration was done in two steps. First the structure contour maps of these two horizons were unfolded. Then we estimated the thrust displacement by interpolation: With the simple rule of flexural folds, on cross sections, we projected above Sespe to interpret the top Modelo hanging wall cutoff, and we projected below Pico to interpret the top Modelo footwall cutoff. We added an area to the map restoration figure (dark gray shading in Figure 5b) which represents the horizontal projection of the distance between the Sespe and the Modelo hanging wall cutoffs, plus the distance between the Pico and the Modelo footwall cutoffs, for the Red Mountain, San Cayetano, and Oak Ridge faults.

5. Results

In most of the cases of the studied area, the UNFOLD fitting indicators are very low; therefore the maps represent developable surfaces, similar to the unfolding of a sheet of paper [*Gratier et al.*, 1991]. Assuming that a constant thickness of layers was maintained during the folding process, low-fitting indicators indicate that the contour maps are accurate, which is not too surprising because of the numerous petroleum wells which constrain the folded areas. In some areas, such as in the Ventura basin, the dip of the strata is very high, and, consequently, the geometry of the folded layer is difficult to depict from wells. In such cases, the fitting indicators are not as good, but none of the studied surfaces had to be considered to be nondevelopable surfaces. The main problem of the restoration is fitting the unfolded block outlines to each other across faults or artificial boundaries. The simplest way is to search for a balance between voids and overlaps between the unfolded blocks. Automatic programs exist for fitting rigid blocks [*Audibert*, 1991; *Rouby et al.*, 1993]. However, depending on the data, some part of the boundary may be better known than others. For example, a well near a fault may impose a strong constraint on the geometry of the boundary. Consequently, the best fitting was done when taking into account the quality of the available data. As in a preceding study using seismic data [*Gratier and Guillier*, 1993], it is found that voids are most often larger than overlaps. This is probably due to the fact that geologists are more likely to miss part of a layer rather than to draw a nonexisting one. Steep or overturned fold limbs might be missed during interpretation, and thrust overlap is more likely to be underestimated than overestimated.

Results for the Ventura and Los Angeles basin are summarized in Figures 4 and 5. Map projections of overlaps and directions of local shortening deduced from the unfolding of

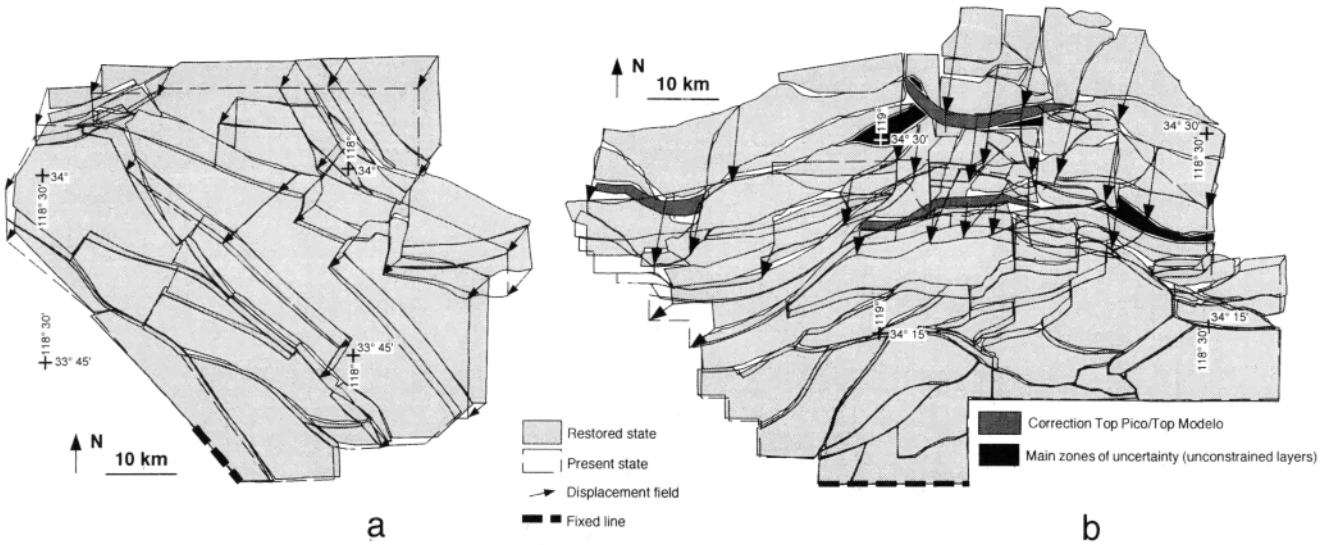

Figure 5. Restored state of the (a) Los Angeles and (b) Ventura basins (see location in Figure 3). The comparison between the restored (initial) state (gray areas) with the deformed (present) state (dashed lines) gives the relative displacement field relative to the southern boundary of each basin since 4–5 Ma. The arrows indicate this displacement and are at the same scale as the map. This restoration includes the effect of folds and faults. The medium gray areas are the zones where corrections for the difference of age of the reference unfolded layers were done. Black areas are the zones where the lack of data prevent us from drawing an accurate geometry of the reference layers.

each block and vertical axis rotations for best fitting the restored block are given in Figure 4. The senses of the rotation appear to be similar in adjacent blocks. The finite displacement field in Figure 5 includes both the effect of folding and faulting.

In the Los Angeles basin the fitting of the unfolded blocks (Figure 5a) was rather easy. For most of the faults, the maximum local void, or overlap distance, is about 200 or 300 m. Thrust displacements are better constrained within the basins, where strata are preserved on both sides of the faults, than at the edge of the basin, were strata are eroded. A higher degree of freedom exists at the edge of the mapped area. Two structures present larger local overlap or void distances after the restoration: the Santa Monica fault and the Whittier fault. However, these local mismatches never exceed half a kilometer. Along cross sections through the entire Los Angeles basin, the ratio between the sum of the voids and overlaps and the total distance never exceeds 2–3%. With the more than 30 fault blocks used here, the position of blocks are constrained by neighbors, especially away from the edges of the restored area. Misfits suggest local misinterpretation of the data, but these misfits are small.

In the Ventura basin the best fitting of the unfolded blocks was not as good as in the Los Angeles basin because of uncertainty on the geometry of steep dip and overturned fold limbs (Figure 5b). The region south of the Oak Ridge-Northridge thrust belt (Figure 3) was restored with the same degree of confidence as was the Los Angeles basin. The results in the northern region were not as good, particularly along the Red Mountain-San Cayetano-Santa Susana thrust belt (Figure 3). Most of the misfits were seen as voids. Local voids (white areas in Figure 5b) reach 1 km. Moreover, in three areas indicated as black in Figure 5b (two areas south of San Cayetano fault and one area south of Santa Susana fault), lack of data prevented us from drawing a reliable geometry of all the faulted blocks. The location of the zones of major misfits (Figure 5b) may be matched with the map projections of the thrust surfaces (Figure 4b): Areas with local problems of compatibility are associated with discontinuous lateral change in the thrust displacement values (San Cayetano) or are associated with the superposition of several thrusts, which successively refolded the preceding (Santa Susana system). These mismatches express the difficulty of drawing folded and faulted layers which are directly balanced in such complex structures. However, the thrust displacement across these zones of major misfits was estimated from adjoining areas along strike where the geometry is well-constrained so that the regional reconstruction is accurate.

In the Santa Barbara Channel basin the fitting was easier than for the Los Angeles basin because dips are gentle over wide areas (Sorlien et al., submitted manuscript, 1998). The first aim of the map restoration has been reached when the areas with a lack of geometrical compatibility are identified. A careful reinterpretation of the geometry of these zones would help us to resolve the local deformation field to understand, for example, the mechanisms of lateral evolution and termination of thrusts and folds. However, from the analysis of the restored blocks (Figure 5), it appears that the constraints imposed on the regional deformation field by the zones, which are well constrained, are strong enough to overcome the problem of the local misfits. It is thus possible to estimate the overall finite crustal deformation of the basins and to draw the associated (relative) displacement field without a second iteration of the procedure.

6. Discussion

The finite deformation of the Los Angeles and Ventura basins is discussed successively referring to both local (Figures 4a and 4b) and regional deformation (Figures 5a and 5b). The local deformation is the shortening and rotation of individual folded blocks. The regional deformation and displacement

field are estimated for each basin with respect to reference lines on the Pacific side of the basins. Then, adding the Santa Barbara Channel area (Sorlien et al., submitted manuscript, 1998) to the Ventura and Los Angeles basins, we discuss the global displacement field of the western Transverse Ranges and vicinity with a single reference line at the southern boundary of the whole area. We propose a regional model of crustal displacement, which allows one to predict the displacement in the zones where data (folded and faulted Mio-Pliocene strata) were not available (e.g., San Gabriel Mountains). Finally, we compare our results with the other geophysical data.

6.1. Finite Deformation of the Los Angeles Basin

The unfolding of the blocks and the fitting of these unfolded blocks gives a NE-SW principal direction of shortening for the Los Angeles basin. Including the effect of folds and faults, regional shortening is ~9% in this direction (Figure 5a and cross section CC′ in Figure 3), with volume being conserved for the most part, by crustal thickening and uplift and not by horizontal extension. The displacement is ~5.4 km and changes in direction from NE-SW, on the eastern margin, to NNE-SSW, on the northern margin of the basin. The dispersion of maximum shortening values, which range from NNW-SSE to NE-SW, revealed the heterogeneity of the deformation (Figure 4a). Both clockwise and counterclockwise local block rotations were needed to best fit the unfolded blocks (Figure 4a). Although the directions of shortening are very reliable, since they are dependent on the well-known geometry of the layer, the values of local rotations are not so well constrained, since these values strongly depend on the geometry of the faulted block boundary. These local rotations must thus be considered as approximate values. Nevertheless, clockwise rotations (2°–5°) are systematically associated with the N-S directions of shortening (northern part of the Los Angeles basin and near the Whittier fault zone). In contrast, counterclockwise rotations were needed near the western part of the basin where there is NE-SW shortening. Very local N-S directions of shortening are also found along the Newport-Inglewood fault associated with E-W-trending, right-stepping en-echelon folds, indicating right-lateral strike-slip displacement along this fault [*Harding*, 1973]. However, this displacement is rather low as late Cenozoic strata are only locally cut through by faults. An en-echelon pattern of several thrusts is associated with NW-SE dextral simple shear along the Elsinore-Whittier fault system (Figure 4a).

Generally, the value of the NNE-SSW total displacement (relative to the fixed Pacific plate, see Figure 6) decreases from northwest (Los Angeles) to southeast. This spatial change of displacement values must be associated with a regional counterclockwise rotation of the northeast boundary of the Los Angeles basin. Large NW-SE thrusts and associated tight folds in east Ventura basin (Figure 4b) indicate a lateral continuation of this scissors motion. This regional counterclockwise rotation is estimated to be 3°–5°.

6.2. Finite Deformation in the Ventura Basin

Restoration of the sedimentary cover of the Ventura basin, including both the fold and fault effects, indicates a mean N-S principal direction of shortening, with an overall regional shortening of ~25% in this direction and 15 km of relative displacement (Figure 5b). The deformation is strongly heterogeneous. Most of the deformation (70%) is accommodated north of the Oak Ridge-Northridge fault system, by north dipping thrusts (Red Mountain, San Cayetano, Santa Susana thrusts, and other blind thrusts) and associated tight folds. The other part of the deformation (30%) is associated with the displacement on the south dipping Oak Ridge and Northridge thrust system (see section AA′ and BB′ in Figure 3). Surprisingly, the thrusts (particularly the north dipping ones such as the Red Mountain and San Cayetano faults) do not define a unique continuous structure in map view (Figure 3). On the contrary, each thrust is an independent structure whose displacement increases progressively from west to east and which ends along tear faults (see Figures 3 and 4). These tear faults guide slip on the thrust faults. The thrust system can be considered threaded [*Thibaut et al.*, 1996]: N-S slip is permitted, oblique slip is blocked, and this is compatible with the result of the restoration. The deformation is accommodated by folds between the thrusts (e.g., zone of folded strata between the Red Mountain and San Cayetano (section BB′ in Figure 3) possibly associated with blind thrusts [*Namson and Davis*, 1988; *Huftile and Yeats*, 1995]. In this case, folding along some sections (BB′ in Figure 3) takes up the same order of magnitude of horizontal shortening as does thrust displacement on neighboring sections (AA′ in Figure 3).

The block south of the Oak Ridge-Northridge fault system is almost rigid and does not accommodate more than a few percent (5%) of the total deformation (Figure 5b). This rigidity may be linked to deep structures (volcanic structures) [*Yeats and Huftile*, 1995] or some other major difference in crustal composition of this domain versus the northern one. The displacement is deflected around this rigid domain which acts as an indenter. This effect is also particularly spectacular along the NE-SW trending part of the Oak Ridge fault where the N-S displacement of the San Cayetano-Red Mountain thrusts is deflected parallel to the fault (Sorlien et al., submitted manuscript, 1998), displacement along the Oak Ridge fault varies from thrust along its E-W-trending part to left-oblique-reverse on its NE-SW trending part. Deviation of the displacement along preexisting normal strike-slip faults appears in the foreland of other mountains ranges such as in the Alps [*Gratier et al.*, 1989].

The analysis of local finite deformation confirms that shortening directions are molded around the rigid domain (Figure 4b). However, the shortening values east of the Ventura basin are much larger than those west of the Ventura basin. Several recent earthquakes (San Fernando and Northridge, with near NNE-SSW directions of dip slip) attest to the continuation of this main direction of regional shortening in the eastern Ventura basin [*Jackson and Molnar*, 1990; *Yeats and Huftile*, 1995] (see Figure 9).

Similarly to the Los Angeles basin, local rotations in the Ventura basin (Figure 4b) were needed to best fit the unfolded blocks (Figure 5b). Again, the reliability of the direction of shortening (based upon folds) is much better than the reliability of the rotations (based on the geometry of the faults). Counterclockwise rotations are found in the eastern part of the Ventura basin which is characterized by NNE-SSW shortening. In contrast, blocks in the West Ventura basin, characterized by NNW-SSE shortening have rotated clockwise.

For compatibility reasons, E-W extension of the material located between the San Cayetano fault and the E-W-trending part of the Oak Ridge fault (Figure 3) is required because of the lateral westward expulsion of Ventura basin along the Oak Ridge fault (associated with the divergence of the displacement vectors (Figure 5b)). There is significant vertical separa-

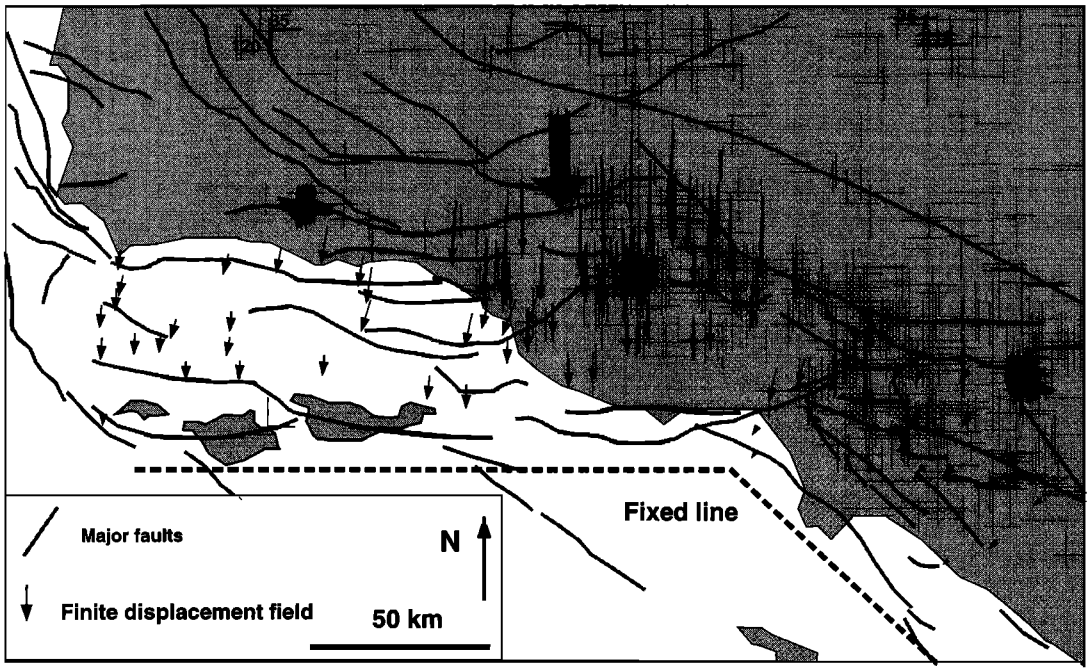

Figure 6. Total finite displacement field for the western Transverse Ranges and vicinity (within the Pacific plate), including the Los Angeles, Ventura, and Santa Barbara basins, relative to the southern boundary of the whole area (fixed line), during the last 4–5 Ma. The arrows indicate this displacement and are at the same scale as the map. The thick shaded arrows indicate the mean displacement directions along the northern boundary of the three basins.

tion of Pico and Saugus formations strata across NE-striking faults in this area, and this zone is also the area of maximum depth for the Plio-Quaternary sediments (near section AA′ (Figure 3)). These faults may be interpreted as normal-separation faults with a component of left-lateral movement. In contrast to this fault-parallel extension in the footwall of the Oak Ridge fault, contraction is needed parallel to the E-W fold trend in the hanging wall of the San Cayetano fault associated with the convergence of the displacement vectors (Figure 5b). The fault-parallel shortening in its hanging wall perhaps contributes to the omega shape of this thrust in map view (Figure 3).

6.3. Regional Finite Displacement and the Proposed "Double Fan Closure" Model

A regional displacement field including the Los Angeles, Ventura, and Santa Barbara basins, is given in Figure 6. This finite displacement is with respect to a reference line along the southern boundary of the whole area. In order to draw this global displacement field, the displacement along the Santa Monica fault-Channel Island faults, which separate the western Transverse Ranges from the California continental borderland (Figure 3), had to be estimated. A large anticline is associated with these thrusts that includes the Santa Monica Mountains and the northern Channel Island structures [*Dibblee*, 1982; *Davis and Namson*, 1994; *Shaw and Suppe*, 1994]. Seeber and Sorlien (submitted manuscript, 1998) recently estimated the displacement on this thrust using cross sections and seismic reflection profiles with a listric fault model. We used a mean value of thrust displacement which ranges from ~3 km (San Miguel Island) to a maximum 9 km in its eastern part (north of Los Angeles). This last value is only slightly lower than the 12.5 km obtained by *Davis and Namson* [1994] with a ramp/flat kink model. The mean direction of displacement on this thrust was considered as parallel to the mean direction of displacement in the Ventura basin. This thrust displacement increases from west to east and implies a clockwise rotation of ~2° between the hanging wall and the footwall. In order to complete the displacement field, the displacement across the northern boundary of the Santa Barbara Channel (North Channel fault (Figure 3)) was also included using a cross section drawn from seismic data, petroleum test wells, and geologic maps: 3.5 km of NNE shortening, near Santa Barbara [*Hornafius et al.*, 1995].

Adding the deformation associated with the Ventura and Santa Barbara Channel basins plus the deformation linked to the Santa Monica fault-Channel Island faults, the regional displacement of the northern boundary of the studied area increases eastward from 5 to 24 km, corresponding to a clockwise rotation of 10°. In order to extrapolate the regional displacement field to areas where post-Miocene sediments are missing we propose a "double fan closure" model of this displacement (Figure 7). For simplicity the elements of the fans are considered as rigid. This model implies a 10° clockwise rotation of the northern boundary of the studied area and a 5° counterclockwise rotation of its northeast boundary. These two rotations fit the restoration results rather well (Figure 8). The values of these two rotations are imposed by the lateral decrease of the displacement values deduced from our restoration. The zone of transition between the two senses of rotation is the zone of the maximum displacement of the Santa Susana fault. Local discrepancies between displacement values deduced from the model of Figure 7 and those inferred from our restoration can be explained by the fact that in contrast to the schematic model of Figure 7 the elements of the fans are not rigid but are slightly deformable in natural deformation. For

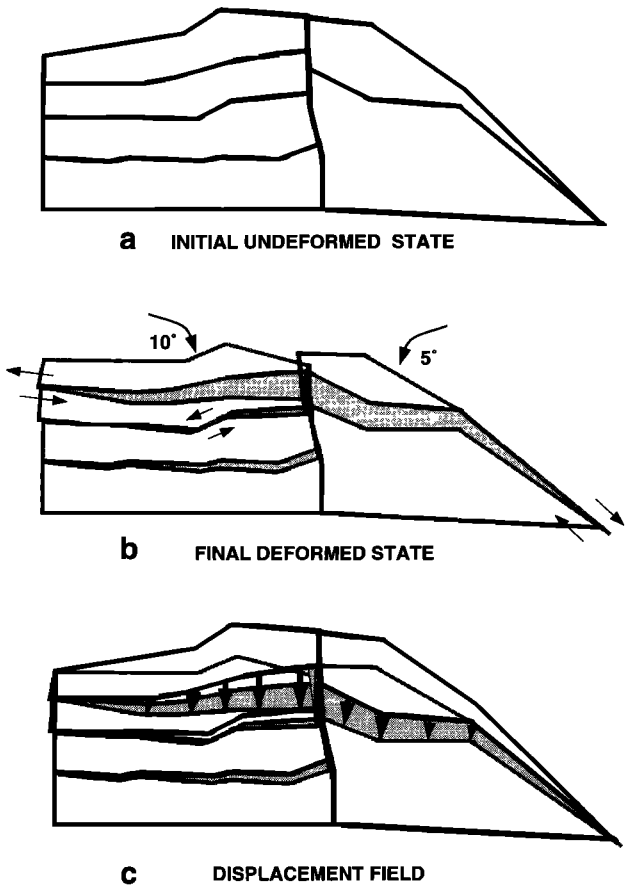

Figure 7. "Double fan closure" model of the crustal deformation of the Western Transverse Ranges, schematic approach with rigid elements for the fans. (a) Restored (undeformed) state, (b) present (deformed) state and associated strike slip or simple shear deformation, and (c) comparison of deformed and undeformed states and total finite displacement field relative to the southern boundary. The shaded area is the zone of maximum shortening accommodated either by thrusts or by folds.

example, solution cleavage indicating internal deformation by pressure solution creep is described near major faults in the Transverse Ranges [*Gratier et al.*, 1994]. To account for the small difference in displacement directions between Los Angeles and east Ventura (Figure 8), the northeastern fan element can be slightly deformed. However, for simplicity, this internal deformation is not introduced in Figure 7.

For compatibility reasons with such a fan model, a slight lateral slip must occur between elements of the fan, and/or they must undergo a small amount of E-W shortening near the northern boundary of the studied area (Figure 7b). Such observations have been discussed related to the Ventura basin finite deformation. For the best fitting, E-W contraction is required in the San Cayetano hanging wall. Left-lateral strike-slip displacement was described on some of the E-W trending faults such as the Santa Ynez fault [*Sylvester and Darrow*, 1979] and the Santa Monica fault [*Truex*, 1976; *Wright*, 1991]. Right-lateral displacement along the northeast NW-striking boundary is registered by en-echelon thrusts, for example south of the Whittier Fault in east Los Angeles basin (Figure 3).

With such a fan model, the amount of rotation varies from place to place as do the rotations of the elements of a fan. The difference with a true fan is that the boundaries between the elements are not perfectly cut. On the contrary, even the major thrust belt (North Channel-Red Mountain-San Cayetano) is made of disconnected thrusts ending by tear faults and with tight folds in the bridges between these thrusts. The reality must thus be a type of fan made of incompletely cut elements which consequently needs to be articulated and deformable.

This model is clearly different from either of the so-called "book shelves sliding" models with pure strike-slip faulting [*Freund*, 1970; *Garfunkel*, 1974; *Luyendyk et al.*, 1980; *Garfunkel and Ron*, 1985] or the model with oblique slip between the blocks (pinned model) [*McKenzie and Jackson*, 1983, 1986], where the rotations are homogeneous through the whole area. However, a fan model may be combined with either these block models (if large sliding occurs along the elements) or with continuous deformation [*Jackson and Molnar*, 1990]. This

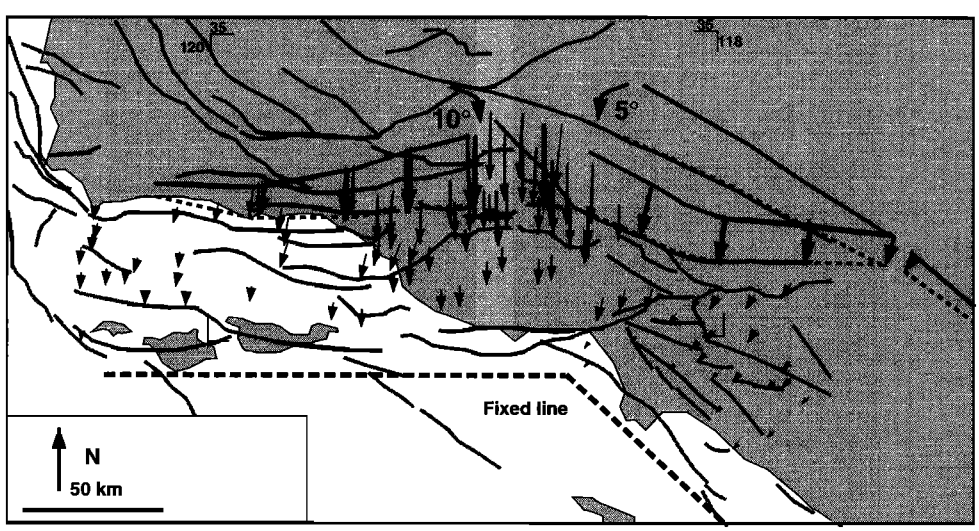

Figure 8. Comparison of the displacement inferred from our restoration (Figure 6) (thin arrows), with the displacement associated with the double fan closure model (Figure 7) (thick arrows). Local discrepancy between the displacement values deduced from the model of Figure 7 and those derived from our restoration can be explain by the fact that in contrast to the schematic model of Figure 7 the elements of the fans are not rigid but partially deformable in natural deformation.

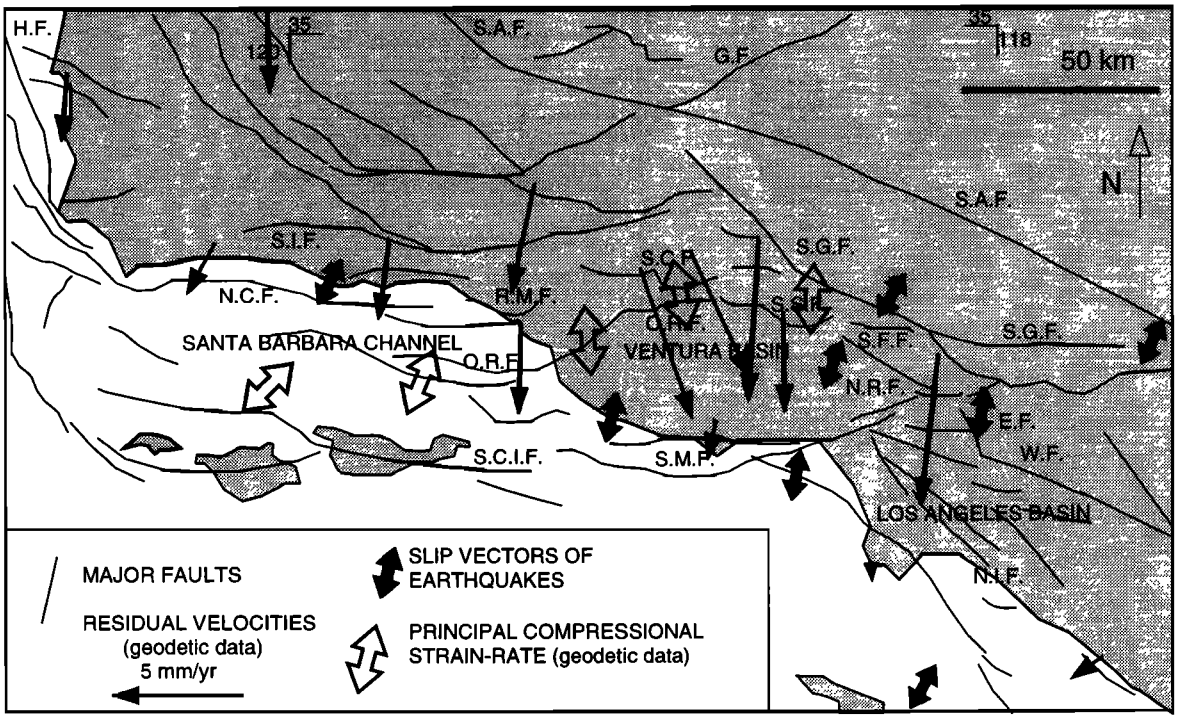

Figure 9. Schematic map view of displacement field and principal compressive strain axes (maximum shortening rate) obtained from geodetic data and fault plane solutions of major earthquakes. The displacement field is the residual velocities (observed geodetic velocity corrected for the effect of the San Andreas fault system) given by *Feigl et al.* [1993]. This displacement field (arrows) may be compared with the displacement derived from the restoration of the strata (Figure 6 and 8), since it is relative to a fixed point in the Pacific plate located along the western part of the fixed line used in Figures 6 and 8. The directions of maximum shortening rate deduced from geodetic data are those given by *Donnellan et al.* [1993]. The azimuths of near-dip-slip vectors of earthquakes are from *Yerkes* [1985], *Jackson and Molnar* [1990], and *Hauksson et al.* [1995]. These two types of data may be compared with the finite deformation of each block given in Figure 4.

could add an homogeneous rotation which cannot be estimated from our study.

The increase in crustal shortening from west to east in the western Transverse Ranges must be related to structures at depth that experienced the same N-S shortening. From subsurface observations, the Ventura basin is the zone of maximum N-S horizontal shortening and is also the zone of maximum subsidence. For example, the depth of the 1 Ma horizon may reach 3–4 km in the basin [*Huftile and Yeats*, 1995, 1996], cross sections AA′ and BB′ in Figure 3. Local thickening of the mantle [*Hadley and Kanamori*, 1977; *Raikes*, 1980; *Humphreys et al.*, 1984] and deep earthquakes [*Bryant and Jones*, 1992] located below the Ventura basin may indicate the zone of maximum N-S shortening at depth.

6.4. Comparison With Other Data for Finite Displacement and Deformation Rate

Our results may be compared with geologic data deduced from other techniques and with geodetic data. For horizons older than 4 Ma, *Huftile and Yeats* [1995, 1996] constructed cross sections across the Santa Susana, San Cayetano, and Red Mountain thrusts with essentially the same geometry as the R. J. Hindle et al. (unpublished document, 1989) cross sections used by us. Therefore it is not surprising that total shortening for pre-4 Ma layers, measured by us from both sets of cross sections using the same fixed and mobile references, would be exactly the same (respectively 11, 15, and 11 km for the thrusts above). *Huftile and Yeats* [1995, 1996] obtained shortening rates of 5.7, 8.3, and 10 mm/yr (for the Santa Susana, San Cayetano, and Red Mountain thrusts, respectively) when using a 0.5 Ma horizon, where we have 2.75, 3.75, and 2.75 mm/yr, respectively (Figure 5b), using the older horizons and a 4 Ma duration. Although there is a lot of extrapolation in the *Huftile and Yeats* [1995, 1996] restorations to account for erosion, it seems likely that deformation rates across the Ventura basin have increased with time.

We have compared the average displacement rates and directions for at least the last 4 m.y. to those for the last few years calculated from GPS data. We used the residual velocity field obtained after correction of the simple shear effect of a locked San Andreas fault by *Feigl et al.* [1993] in Figure 9.

In the Ventura basin and eastern part of Santa Barbara Channel basin, the principal maximum shortening directions deduced from geodetic data [*Donnellan et al.*, 1993; *Larsen et al.*, 1993] (Figure 9) are highly compatible with the directions of finite deformation deduced from unfolding of the blocks (Figure 4). The azimuth of the displacement deduced from geodetic data is near N-S [*Feigl et al.*, 1993] (Figure 9). Our N-S to NNE-SSW direction of finite displacement (relative to the same reference) is thus compatible with these results (Figure 6). However, because of heterogeneity of the geodetic deformation, the comparison of the displacement-rate values is not simple. For example, when comparing the displacement of the block north of the Ventura basin relative to the southern part of the Los Angeles basin including the Santa Monica thrust

system, our restoration gives a total displacement of 24 km (Figure 6) and a velocity of 6 mm/yr, which is within the uncertainty of the geodetic velocities for the same references: 4.6–7 mm/yr [after *Feigl et al.*, 1993]. However, geodetic displacement rates not including the Santa Monica Mountain thrust system are about the same, 5–8 mm/yr [*Larsen et al.*, 1993; *Donnellan et al.*, 1993]. This thrust accommodated up to 9 km of slip since the beginning of the N-S shortening (Figure 6), so current slip rates are now less than the uncertainty of the geodetic data.

In the Los Angeles basin, the matching of the geodetic data with our displacement field is not simple because of the lack of geodetic data near the eastern boundary of the basin. When calculating shortening across the Los Angeles basin most authors estimate the displacement of the San Gabriel Mountain versus the southwest part of the Los Angeles basin [*Davis et al.*, 1989]. In our study, owing to the lack of young strata in the area north of Los Angeles, the displacement of the San Gabriel Mountains is extrapolated from compatibility with neighboring areas, using the double fan model (Figure 8). Our extrapolated value (17.5 km) for the displacement of the San Gabriel Mountains versus the southwestern part of the Los Angeles basin corresponds to a 4.4 mm/yr velocity which is in the range of uncertainty of the geodetic measurements between the same references: 3.8–6.2 mm/yr [after *Feigl et al.*, 1993] (see Figure 9). This 17.5 km displacement deduced from our restoration is close to the minimum estimate of *Davis et al.* [1989]: 15–21.4 km, but it is half their maximum values (30 km) obtained with balanced cross sections based on different structural models. The N-S convergence near the northern Los Angeles basin deduced from our restoration is also compatible with the crustal deformation deduced from the GPS data of *Shen et al.* [1996].

6.5. Comparison With Other Data for Rotation

In most of the western Transverse Ranges a clockwise rotation is found during Neogene time [*Luyendyk et al.*, 1980, 1985; *Kamerling and Luyendyk*, 1985; *Hornafius et al.*, 1986], which is compatible with the sense of our clockwise rotation for the northern boundary of the Santa Barbara-Ventura basins. However, the average rate of this clockwise rotation since 17–19 Ma (5°–6°/m.y. [after *Luyendyk*, 1991]) is higher than the overall rotation deduced from our restoration (2.5°/m.y. near the northern boundary and smaller in the southern part of the Western Transverse Ranges). Locally higher rotation-rate values are inferred from our restoration (Figure 4) which reveals a pattern of heterogeneous structures not in good agreement with a recent homogeneous rotation of the whole western Transverse Ranges. When considering the compatibility of movement of the various blocks, heterogeneous rotation is expected and also appears in the geodetic data [*Feigl et al.*, 1993] and recent paleomagnetic studies [*Liddicoat*, 1992; *Levi and Yeats*, 1993].

A counterclockwise rotation of the Mohave-San Gabriel block has also been inferred both from paleomagnetic and geological studies [*Garfunkel and Ron*, 1985; *Dokka and Travis*, 1990]. This is compatible with our counterclockwise rotation of the eastern boundary of the studied area (Figure 8).

Finally, our results may be compared with focal mechanisms. Fault-plane solutions of major earthquakes have been synthesized by *Yerkes* [1985], *Hauksson* [1990], *Hauksson et al.* [1995], and *Jackson and Molnar* [1990]. The azimuths of near dip-slip vectors vary from N-S to NNE-SSW in the studied area (Figure 9) and are compatible with our inferred direction of maximum crustal shortening in Ventura basin and north of Los Angeles basin (Figure 4).

7. Conclusions

The unfolding of sedimentary layers followed by the best fitting of the restored blocks allows us to reconstruct the initial (undeformed) state of the Los Angeles and Ventura basins prior to the recent period of NNE-SSW shortening. The first result of this map restoration is a test of the map compatibility between the data. The compatibility is found to be good in most of the studied areas, thanks to the thousands of wells incorporated in the structure contour maps. Mismatches are localized in the more complex zones. The problems are ascribed to inadequacies in the available geological and geophysical data. The restoration method reveals the zones with local problems of compatibility where the next studies might be focused.

The constraints imposed on the regional deformation field by the zones which are well constrained are strong enough to overcome the problem of the local misfits. It is thus possible to estimate the overall finite crustal deformation of the Ventura and Los Angeles basins. When integrating the restoration of the Santa Barbara Channel, the finite displacement field for the western Transverse Range is inferred from this restoration method.

The total finite displacement field may be modeled by the effect of the closure of a double fan with partially deformable elements. This model implies a 10° clockwise rotation of the northern boundary of the western Transverse Ranges and a 5° counterclockwise rotation of its northeast boundary (including that of the Los Angeles basin).

Lateral variation of the total finite deformation, both in direction and amount reveals the heterogeneity of the subsurface deformation. Most of the major thrusts appear to initiate as en-echelon structures along the left-lateral northern margin and the right-lateral northeastern margin of the studied area.

The total finite map deformation and displacement values matched well with those obtained by section-balancing techniques or fault slip measurements. However, comparison of the rates of deformation is found to be strongly dependent on the possible evolution of the deformation rate with time and on the extrapolation of the geometry of the youngest partially eroded horizons. With this qualification, our modeled map deformation and displacement values are near the minimum values of balanced cross sections from the San Gabriel Mountains across the Los Angeles basin. Our results are in good overall agreement with geodetic data, paleomagnetic data, and fault plane solutions of major earthquakes. However, local discrepancies emphasize the need for more careful studies of the heterogeneity of the deformation and the partitioning between reversible and irreversible deformation.

Finally, the idea of this work is not to establish a definitive model of the kinematics of southern California. On the contrary, the main interest of the restoration method is to impose geometric and kinematic compatibility between the data. As new data become available, the reconstruction and interpretation can be modified in order to respect these compatibilities.

Acknowledgments. We thank Nano Seeber, Charles DeMets, and John Suppe for constructive and helpful comments, Craig Nicholson for geologic discussions and for getting the Ventura Basin data pur-

chased and placed on the web, and R. J. Hindle and H. E. Stark, the co-authors of the work on the Ventura basin. The funds for the acquisition of the Ventura Basin data set and to establish the website were provided by the U.S. Geological Survey under the National Earthquake Reduction Program (NEHRP). Part of this work was done during the stay of JPG in ICS-UCSB, supported by the SEC Program.

References

Atwater, T., Plate tectonic history of the northeast Pacific Ocean and Hawaii, in *The Eastern Pacific Ocean and Hawaii, The Geology of North America*, vol. N, edited by E. L. Winterer, et al., pp. 21–71, Geol. Soc. of Am., Boulder, Colo., 1989.

Audibert, M., Deformation discontinue et rotation de blocs, *Mem. Docum. C.A.E.S.S. Rennes*, *40*, 1991.

Bird, P., and X. Kong, Computer simulations of California tectonics confirm very low strength of major faults, *Geol. Soc Am. Bull.*, *106*, 159–174, 1994.

Bird, P., and R. W. Rosenstock, Kinematics of present crust and mantle flow in southern California, *Geol. Soc. Am. Bull.*, *95*, 946–957, 1984.

Blake, G. H., Review of the Neogene biostratigraphy and stratigraphy of the Los Angeles Basin and implications for basin evolution, in *Active Margin Basins*, edited by K. T. Biddle, *Mem. Am. Assoc. Pet. Geol.*, *52*, 135–184, 1991.

Bryant, A. S., and L. M. Jones, Anomalously deep crustal earthquake in the Ventura basin, southern California, *J. Geophys. Res.*, *97*, 437–447, 1992.

Clark, D. H., N. T. Hall, D. H. Hamilton, and R. G. Heck, Structural analysis of late neogene deformation in the central offshore Santa Maria Basin, California, *J. Geophys. Res.*, *96*, 6435–6457, 1991.

Cobbold, P. R., Removal of finite deformation using strain trajectories, *J. Struct. Geol.*, *1*, 67–72, 1979.

Cobbold, P. R., and M. N. Percevault, Spatial integration of strain trajectories, *J. Struct. Geol.*, *5*, 299–305, 1983.

Crouch, J. K., and J. Suppe, Late Cenozoic tectonic evolution of the Los Angeles basin and inner California borderland: A model for core complex-like crustal extension, *Geol. Soc. Am. Bull.*, *105*, 1415–1434, 1993.

Crowell, J. C., An outline of the tectonic history of southeastern California, *The Geotectonic Development of California*, Rubey vol. 1, edited by W. G. Ernst, pp. 583–600, Prentice Hall, Englewood Cliff, N. J., 1981.

Dahlstrom, C. D. A., Balanced cross-sections, *Can. J. Earth Sci.*, *6*, 743–757, 1969.

Davis, T. L., and J. S. Namson, A balanced cross section of the 1994 Northridge earthquake, southern California, *Nature*, *372*, 167–169, 1994.

Davis, T. L., J. S. Namson, and R. F. Yerkes, A cross section of the Los Angeles area: Seismically active fold and thrust belt, the 1987 Whittier Narrows earthquake and earthquake hazard, *J. Geophys. Res.*, *94*, 9644–9664, 1989.

Dibblee, T. W., Geology of the Santa Monica Mountains and Simi Hills, southern California, in *Geology and Mineral Wealth of the California Transverse Ranges*, Mason Hill Vol., pp. 94–130, South Coast Geol. Soc., Santa Ana, Calif., 1982.

Dokka, R. K., and C. J. Travis, Late Cenozoic strike slip faulting in the Mohave desert, California, *Tectonophysics*, *9*, 311–340, 1990.

Donnellan, A. B., B. H. Hager, R. W. King, and T. A. Herring, Geodetic measurements of deformation in the Ventura basin region, southern California, *J. Geophys. Res.*, *98*, 21,727–21,739, 1993.

Dumont, M. P., and J. A. Barron, Diatom biochronology of Sisquoc Formation in the Santa Maria basin, California, and its paleooceanographic and tectonic implications, in *Evolution of Sedimentary Basins, Onshore Oil and Gas Investigations, Santa Maria Province*, edited by M. A. Keller, *U.S. Geol. Surv. Bull.*, *96-01941*, K1-7, 1995.

Edward, E. B., and R. G. Heck, Structural model for Gato Canyon field, Santa Barbara Channel California, *Am. Assoc. Pet. Geol. Bull.*, *78*, 662, 1994.

Etchecopar, A., Plane kinematic model of progressive deformation in a polycrystalline aggregate, *Tectonophysics*, *39*, 121–139, 1977.

Feigl, K. L., et al., Space geodetic measurements of crustal deformation in central and southern California, 1984–1992, *J. Geophys. Res.*, *98*, 21,677–21,712, 1993.

Freund, R., Rotation of strike slip faults in Sistan Southeastern Iran, *J. Geol.*, *78*, 188–200, 1970.

Garfunkel, Z., Model for late Cenozoic tectonic history of the Mohave desert, California, and its relation to adjacent regions, *Geol. Soc. Am. Bull.*, *85*, 1931–1944, 1974.

Garfunkel, Z., and H. Ron, Block rotation and deformation by strike slip faults: The properties of a type of macroscopic discontinuous deformation, *J. Geophys. Res.*, *90*, 8589–8602, 1985.

Gratier, J. P., and B. Guillier, Compatibility constraints on folded and faulted strata and calculation of the total displacement using computational restoration (UNFOLD program), *J. Struct. Geol.*, *15*, 391–402, 1993.

Gratier, J. P., G. Ménard, and R. Arpin, Strain-displacement compatibility and restoration of the Chaînes Subalpines of the Western Alps, in *Alpine Tectonics*, edited by M. P. Coward, D. Dietrich and R. G. Park, *Geol. Soc. Lond. Spec. Publ.*, *45*, 65–81, 1989.

Gratier, J. P., B. Guillier, A. Delorme, and F. Odonne, Restoration and balance of a folded and faulted surface by best-fitting of finite elements: Principle and applications, *J. Struct. Geol.*, *13*, 111–115, 1991.

Gratier, J. P., T. Chen, and R. Hellmann, Pressure solution as a mechanism for crack sealing around faults, natural and experimental evidence, in *Mechanical Involvement of Fluids in Faulting*, edited by S. Hichkmann, R. Sibson, and R. Bruhn, *U.S. Geol. Surv. Open File Rep.*, *228*, 279–300, 1994.

Hadley, D., and H. Kanamori, Seismic structure of the Transverse ranges, California, *Geol. Soc. Am. Bull.*, *88*, 1469–1478, 1977.

Harding, T. P., Newport-Inglewood trend, California: An example of wrenching style of deformation, *Am. Assoc. Pet. Geol. Bull.*, *57*, 97–116, 1973.

Hauksson, E., Earthquakes faulting and stress in the Los Angeles basin, *J. Geophys. Res.*, *95*, 15,365–15,394, 1990.

Hauksson, E., L. M. Jones, and K. Hutton, The 1994 Northridge earthquake sequence in California: Seismological and tectonic aspect, *J. Geophys. Res.*, *100*, 12,335–12,355, 1995.

Hopps, T. E., H. E. Stark, and R. J. Hindle, Subsurface data in basin analysis: An example from Ventura Basin, California, paper presented at Southern California Earthquake Center Workshop: Thrust Ramps and Detachment Faults in the Western Transverse Ranges, Univ. of Calif., Santa Barbara, 1995.

Hornafius, J. S., B. P. Luyendyk, R. R. Terres, and J. J. Kamerling, Timing and extent of Neogene tectonic rotation in the Western Transverse Ranges, California, *Geol. Soc. Am. Bull.*, *97*, 1476–1487, 1986.

Hornafius, J. S., M. J. Kamerling, and B. P. Luyendyk, Seismic mapping of the North Channel Fault near Santa Barbara, Progress Rep., South. Calif. Earthquake Cent., Los Angeles, Calif., 1995.

Hossack, J. R., The use of balanced cross-sections in the calculation of orogenic contraction: A review, *J. Geol. Soc. London*, *136*, 705–711, 1979.

Huftile, G. H., and R. S. Yeats, Convergence rates across a displacement transfer zone in the western Transverse Ranges, Ventura basin, California, *J. Geophys. Res.*, *100*, 2043–2067, 1995.

Huftile, G. H., and R. S. Yeats, Deformation rates across the Placerita (Northridge M = 6.7 aftershock zone) and Hopper Canyon segments of the Western Transverse Ranges Deformation belt, *Bull. Seismol. Soc. Am.*, *86*, 3–18, 1996.

Hummon, C., C. L. Schneider, R. S. Yeats, J. F. Dolan, K. E. Sieh, and G. H. Huftile, Wilshire fault: Earthquakes in Hollywood?, *Geology*, *22*, 291–294, 1994.

Humphreys, E. D., and R. J. Weldon, Deformation across the western United States: A local estimate of Pacific-North American transform deformation, *J. Geophys. Res.*, *99*, 19,975–20,010, 1994.

Humphreys, E., R. W. Clayton, and B. H. Hager, A tomographic image of mantle structures beneath southern California, *Geophys. Res. Lett.*, *11*, 625–627, 1984.

Jackson, J., and P. Molnar, Active faults and block rotation in the Western Transverse Ranges, *J. Geophys. Res.*, *95*, 22,073–22,087, 1990.

Kamerling, M. J., and B. P. Luyendyk, Paleomagnetism and Neogene tectonics of the northern Channel Islands, California, *J. Geophys. Res.*, *90*, 12,485–12,502, 1985.

Larsen, S. C., D. C. Agnew, and B. H. Hager, Strain accumulation in the Santa Barbara channel 1970–1988, *J. Geophys. Res.*, *98*, 2119–2134, 1993.

Larson, K. M., and F. H. Webb, Deformation in the Santa Barbara channel from GPS measurements 1987–1991, *Geophys Res. Lett.*, *19*, 1491–1494, 1992.

Levi, S., and R. S. Yeats, Paleomagnetic constraints on the initiation of uplift on the Santa Susana fault, Western Transverse Ranges, California, *Tectonics*, *12*, 688–702, 1993.

Liddicoat, J. C., Paleomagnetism of the Pico formation, Santa Paula creek, Ventura basin, California, *Geophys. J. Int.*, *110*, 267–275, 1992.

Lonsdale, P., Structural patterns of the Pacific floor offshore of Peninsula California, in *Gulf and Peninsula Province of the California*, edited by J. P. Dauphin and B. T. Simoneit, *Am. Assoc. Pet. Geol. Mem.*, *47*, 87–125, 1991.

Luyendyk, B. P., A model for Neogene crustal rotation, transtension and transpression in southern California, *Geol. Soc. Am. Bull.*, *103*, 1528–1536, 1991.

Luyendyk, B. P., M. J. Kamerling, and R. R. Terres, Geometric model for Neogene clockwise rotation in southern California, *Geol. Soc. Am. Bull.*, *91*, 211–217, 1980.

Luyendyk, B. P., M. J. Kamerling, R. R. Terres, and J. S. Hornafius, Simple shear of southern California during Neogene time suggested by paleomagnetic declinations, *J. Geophys. Res.*, *90*, 12,454–12,466, 1985.

McGroder, M., C. Millson, and D. Gardner, Timing and geometry of left-slip faulting and compressional folding in Hondo field, western Santa Barbara Channel, *Am. Assoc. Pet. Geol. Bull.*, *78*, 670, 1994.

McKenzie, D., and J. Jackson, The relation between strain-rates, crustal thickening, paleomagnetism, finite strain and fault movements within a deforming zone, *Earth Planet. Sci. Lett.*, *65*, 182–202, 1983.

McKenzie, D., and J. Jackson, A block model of distributed deformation by faulting, *J. Geol. Soc. London*, *143*, 349–355, 1986.

Molnar, P., Final report to the Southern California Earthquake Center for work performed during the period from September through December 1991, *S.C.E.C.* Internal Rep., 126 p., Univ. of Calif., Los Angeles, 1993.

Namson, J., and T. Davis, Structural transect of the Western Transverse Ranges, California: Implications for lithospheric kinematics and seismic risk evaluation, *Geology*, *16*, 675–679, 1988.

Nicholson, C., C. C. Sorlien, T. Atwater, J. C. Crowell, and B. P. Luyendyk, Microplate capture, rotation of the Western Transverse Ranges and initiation of the San Andreas transform as a low-angle fault system, *Geology*, *22*, 491–495, 1994.

Nicholson, C., M. J. Kamerling, and T. E. Hopps, 3D subsurface structure of the Ventura basin: Analysis of active fault and fold development in oblique convergence, *Eos Trans. AGU*, *78*(46), Fall Meet. Suppl., F632, 1997.

Oertel, G., Unfolding of an antiform by reversal of observed strains, *Geol. Soc. Am. Bull.*, *85*, 445–450, 1974.

Powell, R. E., Balanced palinspastic reconstruction of pre-late Cenozoic paleogeology, Southern California: Geologic and kinematic constraints on evolution of the San Andreas faults system, in *The San Andreas Fault System: Displacement, Palinspatic Reconstruction and Geologic Evolution*, edited by R. E. Powell, R. J. Weldon, and J. C. Matti, *Geol. Soc. Am. Mem.*, *178*, 1–106, 1993.

Raikes, S. A., Regional variation in upper mantle structures beneath southern California Geophys, *J. R. Astron. Soc.*, *63*, 187–216, 1980.

Ramsay, J. G., *Folding and fraturing of rocks*, p. 568, McGraw-Hill, New York, 1967.

Rouby, D., P. R. Cobbold, P. Szatmari, S. Demercian, D. Coelho, and V. A. Rici, Least-squares palinspastic restoration of regions of normal faulting: Application to the Campos basin (Brasil), *Tectonophysics*, *221*, 439–452, 1993.

Schneider, C. L., C. Hummon, R. S. Yeats, and G. L. Huftile, Structural evolution of the northern Los Angeles basin, California, based on growth strata, *Tectonics*, *15*, 341–355, 1996.

Schwerdtner, W. M., Geometric interpretation of regional strain analysis, *Tectonophysics*, *39*, 515–531, 1977.

Shaw, J. H., and J. Suppe, Active faulting and growth folding in the eastern Santa Barbara Channel, California, *Geol. Soc. Am. Bull.*, *106*, 607–626, 1994.

Shen, Z. K., D. D. Jackson, and B. X. Ge, Crustal deformation across and beyond the Los Angeles basin from geodetic measurements, *J. Geophys. Res.*, *101*, 27,957–27,980, 1996.

Sorlien, C. C., C. Nicholson, and B. P. Luyendyk, Miocene extension and post-Miocene transpression offshore of south-central California, edited by M. Keller, U.S. Geol. Surv. Bull., in press, 1995.

Suppe, J., Geometry and kinematics of fault-bend folding, *Am. J. Sci.*, *283*, 648–721, 1983.

Sylvester, A. G., and A. C. Darrow, Structure and neotectonics of the western Santa Ynez fault system in southern California, *Tectonophysics*, *52*, 389–409, 1979.

Thibaut, M., J. P. Gratier, M. Léger, and J. M. Morvan, An inverse method for determining three-dimensional fault geometry with thread criterion: Application to strike-slip and thrust faults (Western Alps and California), *J. Struct. Geol.*, *18*, 1127–1138, 1996.

Truex, J. N., Santa Monica and Santa Ana Mountains relation to Oligocene Santa Barbara basin, *Am. Assoc. Pet. Geol. Bull.*, *60*, 65–86, 1976.

Weldon, R. J., and E. Humphreys, A kinematic model of southern California, *Tectonics*, *5*, 33–48, 1986.

Weldon, R. J., K. E. Meisling, and J. Alexander, A speculative history of the San Andreas fault in the Central Transverse Ranges, California, in *The San Andreas Fault System: Displacement, Palinspatic Reconstruction and Geologic Evolution*, edited by R. E. Powell, R. J. Weldon, and J. C. Matti, *Geol. Soc. Am. Mem.*, *178*, 161–198, 1993.

Wessel, P., and W. H. F. Smith, Free software helps map and display data, *Eos Trans. AGU*, *72*, 441, 1991.

Wright, T. L., Structural geology and tectonic evolution of the Los Angeles basin California, in *Active Margin Basins*, edited by K. T. Biddle, *Mem. Am. Assoc. Pet. Geol.*, *52*, 35–134, 1991.

Yeats, R. S., Late Quaternary slip rate on the Oak Ridge fault, Transverse Ranges, California: Implications for seismic risk, *J. Geophys. Res.*, *93*, 12,137–12,149, 1988.

Yeats, R. S., and G. F. Huftile, The Oak Ridge fault system and the 1994 Northridge earthquake, *Nature*, *373*, 418–420, 1995.

Yeats, R. S., G. F. Huftile, and L. T. Stitt, Late Cenozoic tectonics of the East Ventura basin, Transverse Ranges, California, *Am. Assoc. Pet. Geol. Bull.*, *78*, 1040–1074, 1994.

Yerkes, R. F., Geologic and seismologic setting, in *Evaluating Seismic Hazards in the Los Angeles Basin Region*, edited by J. I. Ziony, *U.S. Geol. Surv. Prof. Paper*, *1360*, 25–42, 1985.

J. P. Gratier, LGIT, CNRS-Observatoire, Université Joseph Fourier, IRIGM BP 53X, 38041 Grenoble, France. (gratier@obs.ujf-grenoble.fr)

T. Hopps, Rancho Energy Consultants, 250 S. Hallock Drive, Santa Paula, CA 93069.

C. Sorlien, Institute for Crustal Studies, University of California, Santa Barbara, CA 93106.

T. Wright, 136 Jordan Avenue, San Anselmo, CA 94960.

(Received September 30, 1997; revised September 3, 1998; accepted October 2, 1998.)